Results in Physics 6 (2016) 449–455

Contents lists available at ScienceDirect

Results in Physics

journal homepage: www.journals.elsevier.com/results-in-physics

Effect of PbO on the elastic behavior of $ZnO–P_2O_5$ glass systems

H.A.A. Sidek [a,c,*], R. El-Mallawany [b], K.A. Matori [a,c], M.K. Halimah [a]

[a] Ceramic and Ultrasonic Research Laboratory (CURL), Department of Physics, Faculty of Science, Universiti Putra Malaysia, 43400 Serdang, Selangor, Malaysia
[b] Department of Physics, Faculty of Science, Menofia University, Shebin Al-Koam, Egypt
[c] Materials Synthesis and Characterization Laboratory, Institute of Advance Technology (ITMA), Universiti Putra Malaysia, 43400 Serdang, Selangor, Malaysia

ARTICLE INFO

Article history:
Received 12 July 2016
Accepted 31 July 2016
Available online 4 August 2016

Keywords:
Elastic moduli
Glasses
Zinc phosphate
Bond compression
Makishima–Mackenzie models

ABSTRACT

A series of ternary phosphate glasses in the form of $40(P_2O_5)–(60-x)ZnO–xPbO$ and $50(P_2O_5)–(50-x)ZnO–xPbO$ where x = 0–60 mol%, have been successfully prepared by conventional melt quenching technique. Both longitudinal and shear ultrasonic velocities were measured in different compositions of PbO using the MBS8000 ultrasonic data acquisition system at 10 MHz frequency and at room temperature. The ultrasonic velocity data, the density and the calculated elastic moduli are found to be composition dependent and discussed in terms of PbO modifiers. The correlation of elastic moduli with the atomic packing density of these glasses was discussed. To predict the compositional dependence of elastic moduli of this glass system, the interpretation of the variation in the experimental elastic behavior observed has been studied based on various of the bond compression and the Makishima–Mackenzie models.

Introduction

A number of researches have been carried out to improve the physical properties and the chemical durability of phosphate glasses by adding different metal oxides. For example, adding of iron oxide to phosphate glasses could improve the chemical durability and made the glass suitable for storage media for nuclear waste, etc. [1–3]. Yet, the addition of (Fe_2O_3) has been found to change the color of the glass from brown to black and making them of less use for optical applications in the visible region. Other metal oxides like, CaO, ZnO, Al_2O_3, Ga_2O_3, TiO_2, MnO, In_2O_3, Sc_2O_3, etc., were added and found to be good stabilizers of lead phosphate glasses [4–11]. The non-linear optical effects of such glasses resemble of other PbO complex glasses doped with rare earth ions [12–14]. Conversely, the deprived chemical durability, high hygroscopic and volatile nature of lead phosphate glasses disallowed them from replacing the commercial glasses in a wide range of technological applications.

The addition of As_2O_3 to $PbO–P_2O_5$ glasses may further improve the optical transparency in the blue region [15,16]. As_2O_3 is a strong network former [17] and is expected to affect the infrared transmission of P_2O_5 glasses to a less extent, since the frequencies of some of the fundamental modes of vibration of As_2O_3 structural groups lie in the region of vibration of phosphate structural groups [18]. In view of this, it is also expected that As_2O_3 groups form a single arsenic–phosphorus–oxygen framework and may strengthen its structure. The addition of As_2O_3 to these glasses, further, makes them suitable for the long distance optical transmission with low loss and for active fiber Raman amplification [19].

This present work is focused on the lead zinc phosphate glasses where due to their low glass transition temperatures and high thermal expansion coefficient, they are useful for glass-to-metal sealing applications [20,21]. Recently, elastic properties of lead phosphate glass using an ultrasonic technique, ultrasonic and infrared measurements of copper-doped sodium phosphate glasses, and prediction of acoustical properties of phosphate-based glasses have been reported [22–24]. The specific applications of these ternary (PbO)–(ZnO)–(P_2O_5)-glasses make challenging the knowledge of their structure–properties relationships. The prime goal of the present work is to complete the study that was done on the mechanical properties of glasses from phosphate glasses added with PbO and ZnO using ultrasonic pulse-echo method. The compositional dependence of elastic moduli of this glass system is further analyzed using the bond compression and the Makishima–Mackenzie models.

Experimental work

Glass preparation

The systematic series of $(PbO)_x(ZnO)_{60-x}(P_2O_5)_{40}$ and $(PbO)_x(ZnO)_{50-x}(P_2O_5)_{50}$ glasses were prepared by weighing and mixing

* Corresponding author at: Ceramic and Ultrasonic Research Laboratory (CURL), Department of Physics, Faculty of Science, Universiti Putra Malaysia, 43400 Serdang, Selangor, Malaysia.
E-mail address: sidek@upm.edu.my (H.A.A. Sidek).

http://dx.doi.org/10.1016/j.rinp.2016.07.014
2211-3797/

a stoichiometric mixture of lead oxide, PbO (98.0% purity), zinc oxide, ZnO (99.0% purity) and phosphorus pentoxide, P_2O_5 (98.5% purity) in a 50 ml porcelain crucible. The 20 g baches of each glass samples were then weighed using an electronic digital weighing machine with an accuracy of ±0.0001 g. During the process of heating, care must be taken to minimize or avoid the loss of P_2O_5 by having two separate heating stages using two electric furnaces. The crucible was placed into the first electric furnace with temperature of 450 °C for 40 min to evaporate any water vapor trapped in the mixture. The crucible was then transferred to the second electric furnace which was heated at 1000 °C for 80 min, so that a chemical reaction occurred rapidly. However, the exact melting temperature – depended on the glass composition. The crucible was shaken every 15 min to increase the bubble acceleration rate because gas bubbles would be trapped in the viscous mixture throughout the process of heating. Before the melt was poured into the stainless steel split mold, the cylindrical-shaped mold with 20 mm in height, 20 mm in external diameter and 10 mm internal diameter had to be free from dust and impurities by polishing it using sandpaper (ranging coarse grains to fine grains) and then using acetone to clean and wash it. The glass sample was then transferred to the furnace 1 and annealed at 400 °C for one hour to prevent the sample from cracking. After one hour, furnace 1 was switched off and the glass sample was left inside before it was taken out.

The glass samples prepared were kept in plastic bags containing silica gel that acted as a moisture absorption agent and stored in a desiccator to prevent moisture contamination. The cavities that appeared on the surfaces of the sample must be removed to prevent inaccuracy in measurements. Both the surfaces of the sample were cut about 8–10 mm in thickness using a diamond cutter for ultrasonic measurement. Samples were polished using sandpapers of grade 80 (fine grains) – grade 1500 (fine grains) and then cleaned with acetone. A digital vernier caliper (with accuracy ±0.01 mm) was used to check on the thickness of the samples.

Density measurement

The glass's densities were measured at room temperature (23–25 °C) by the Achimedes' method, using acetone as the immersion liquid. Acetone was chosen as a floatation fluid because it has low surface tension. Due to this reason, it will discourage air bubbles from adhering to the sample during immersion. Furthermore, it will not react with or be absorbed by the glass samples. Samples were weighted in air and in acetone by using an electronic weighing machine with an accuracy of ±0.01 g. The density of each annealed glass was measured at room temperature by means of Archimedes technique with acetone as the reference liquid. The sensitivity of the digital weighing machine used was ±0.001 g.

Ultrasonic velocity measurements

The ultrasonic wave velocities V (in m/s) propagated in the glasses were obtained at room temperature, using pulse-echo technique, by measuring the elapsed time between the initiation and the receipt of the pulse appearing on the screen of MATEC Model MBS8000 DSP (ultrasonic digital signal processing) system with 5 MHz resonating frequency [22]. Burnt honey was used as bonding material between X-cut and Y-cut transducers (for generating and detecting the longitudinal and shear ultrasonic waves, respectively), and glass sample. The pulser section generates electrical pulses that are converted into ultrasonic signals using matched transducers. The ultrasonic pulse travels through the specimen bonded to the transducer and an echo is registered each time and returns to the transducer. The amplitude of the successive echoes decreases exponentially due to attenuation in the sample and multiple echoes are observed on the screen. Both longitudinal and shear ultrasonic wave velocities can be calculated using sample thickness and the time interval. The measurements were repeated three times to check the reproducibility of the data. The estimated accuracy of the velocity measurement is about 0.04%.

Results and discussions

Two series of ternary phosphate batch added with PbO and ZnO were melted successfully and formed into a glass. All the glasses were transparent, bubble-free, and homogeneous. The X-ray diffraction patterns of the studied glasses show no discrete or continuous sharp peaks, but the characteristic halo of the amorphous solids. The density (ρ), molar volume (V_m) longitudinal (V_l) and transverse (V_s) ultrasonic velocities of all glasses studied are reported in Table 1.

Density and molar volume

Fig. 1 shows the variation of density and molar volume for both glass series as a function of PbO content (mol%). From Table 1, it can be seen that the density increases gradually as the weight fraction of PbO increases from 0 to 60 mol%. The densities of these glasses are generally high and ranged from 3281 to 5732 kg m^{-3} of glass A: 40(P_2O_5)–(60 − x)ZnO–xPbO and increased from 3177 to 4845 kg m^{-3} for glass B: 50(P_2O_5)–(50 − x)ZnO–xPbO. The molar volume of the glass samples (V_m) was calculated using Eq. (1).

$$V_m = \frac{M_{glass}}{\rho_{glass}} \ (\mathrm{cm}^3) \tag{1}$$

$$M_{glass} = 0.4M_{P_2O_5} + 0.6M_{ZnO} + (x)M_{PbO} \tag{2}$$

where M_{glass} and ρ_{glass} are the mass and density of the glass sample respectively. Molar volume of these glasses is generally decreased and ranged from 37.97 to 33.42 cm^{-3} of glass A: 40(P_2O_5)–(60 − x)ZnO–xPbO and decreased from 36.24 to 30.55 cm^{-3} for glass B: B: 50(P_2O_5)–(50 − x)ZnO–xPbO.

The linear increase of density is due to the heavier lead atomic mass and the low zinc coordination number. The atomic mass and ionic radius of P atom are 30.9737 g and 0.44 Å, Pb (207.2 g and 1.19 Å), O (15.999 g and 1.40 Å) and Zn atoms, which has atomic mass 65.37 g and ionic radius 0.74 Å. The increase in density is also attributed to the formation of new linkages with the addition of ZnO that contributes to a volume contraction. The Pb^{2+} tends to occupy interstitial sites within the highly open glass network.

Table 1
Experimental values of density, longitudinal, shear ultrasonic wave velocity and elastic moduli of glass A: 40(P_2O_5)–(60 − x)ZnO–xPbO and glass B: 50(P_2O_5)–(50 − x)ZnO–xPbO.

Glass sample	P_2O_5	ZnO	PbO	Density, ρ	Molar volume	Longitudinal, V_l	Shear, V_s
	mol%			(kg m^{-3})	(cm^{-3})	(ms^{-1})	
460	40	60	0	3281	37.97	4376	2506
451	40	50	10	3975	39.52	4171	2197
442	40	40	20	4599	40.07	3852	2053
433	40	30	30	4801	37.23	3658	1990
424	40	20	40	5109	35.69	3259	1827
415	40	10	50	5469	34.76	3043	1778
406	40	0	60	5732	33.42	2873	1632
550	50	50	0	3177	36.24	4237	2393
541	50	40	10	3493	34.30	3809	2215
532	50	30	20	4121	35.52	3711	2129
523	50	20	30	4419	33.94	3585	1976
514	50	10	40	4802	33.26	3423	1915
505	50	0	50	4845	30.55	3278	1710

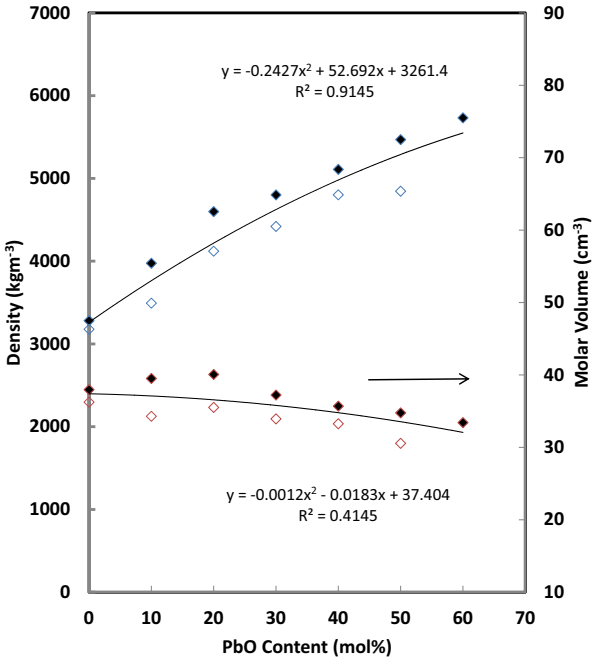

Fig. 1. Density and molar volume of A: 40(P_2O_5)–(60 – x)ZnO–xPbO – First Series (filled diamond) and B: 50(P_2O_5)–(50 – x)ZnO–xPbO – Second Series (open diamond).

Therefore, a greater mass exists in just a slightly decreased molar volume, and hence the density increases.

Ultrasonic velocities and elastic moduli

Fig. 2 shows longitudinal velocity V_l and shear velocity V_s of glasses revealing that the longitudinal and shear velocity decreased with increasing PbO content. The longitudinal (V_l) ultrasonic velocity of glass A: 40(P_2O_5)–(60 – x)ZnO–xPbO, (first series, filled diamond) decreased from 4376 to 2873 m/s and it decreased from 4237 to 3278 m/s for glass B: 50(P_2O_5)–(50 – x)ZnO–xPbO, (second series, open diamond). Also, the shear (V_s) ultrasonic velocity of glass A: 40(P_2O_5)–(60 – x)ZnO–xPbO, (first series, filled

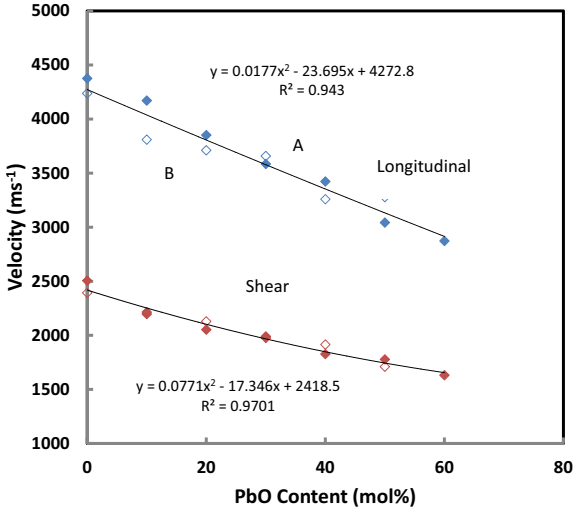

Fig. 2. Longitudinal and shear ultrasonic velocities of A: 40(P_2O_5)–(60 – x)ZnO–xPbO – First Series (filled diamond) and B: 50(P_2O_5)–(50 – x)ZnO–xPbO – Second Series (open diamond).

square) decreased from 2506 to 1632 m/s and it decreased from 2393 to 1710 m/s for glass B: 50(P_2O_5)–(50 – x)ZnO–xPbO, (second series, open square). Elastic moduli (longitudinal (L), shear (G), bulk (K), and Young's (E)) as well as the micro hardness (H), and Poisson's ratio (σ) of the prepared zinc phosphate glasses doped with different percentage of PbO have been determined from the measured ultrasonic wave velocities and density using the relations

$$L = \rho v_l^2 \tag{3}$$

$$G = \rho v_s^2 \tag{4}$$

$$K = L - \left(\frac{4}{3}\right)G \tag{5}$$

$$E = 2(1+\sigma)G \tag{6}$$

$$\sigma = \frac{(L-2G)}{2(L-G)} \tag{7}$$

$$H = (1-2\sigma)\frac{E}{6(1+\sigma)} \tag{8}$$

where ρ is the density (g cm^{-3}), v_l and v_s are the measured longitudinal and shear ultrasonic velocities respectively. Elastic moduli (L, E, K and G) of the studied glasses have been collected in Table 2 and represented in both Fig. 3A for glass A: 40(P_2O_5)–(60 – x)ZnO–xPbO and Fig. 3B for glass B: 50(P_2O_5)–(50 – x)ZnO–xPbO. Elastic moduli (L, E, K and G) for glass A: 40(P_2O_5)–(60 – x)ZnO–xPbO decreased with increasing content of PbO as shown in Fig. 3A, while they also generally decrease for glass B: 50(P_2O_5)–(50 – x)ZnO–xPbO with increasing content of PbO as shown in Fig. 3B. Also, Table 2 collected values of both micro hardness (H) and Poisson's ratio (σ) of the prepared glasses. Microhardness decreased for both glass A: 40(P_2O_5)–(60 – x)ZnO–xPbO and for glass B: 50(P_2O_5)–(50 – x)ZnO–xPbO as the PbO content increased, while Poisson's ratio increased and decreased for glass A and increased for glass B with increasing the PbO content. As seen, from Table 2, all the elastic moduli values decreased with increasing PbO. All the elastic moduli variations in glass composition are similar to the variation of ultrasonic velocity with composition, but Poisson's ratio is opposite, that is, Poisson's ratio increased with the increasing PbO concentration. Poisson's ratio is defined as the ratio between lateral and longitudinal strain produced when tensile force is applied. For tensile stresses applied parallel to the chains, the produced longitudinal strain will be the same and is unaffected by the crosslink density (as explained in the next section), while lateral strain is

Table 2
Experimental values of elastic moduli of glass A: 40(P_2O_5)–(60 – x)ZnO–xPbO and glass B: 50(P_2O_5)–(50 – x)ZnO–xPbO.

Glass sample	Elastic constants (GPa)				Poisson's ratio	Hardness
	L	G	K	E	σ	H (GPa)
460	62.83	20.60	35.36	51.76	0.26	3.35
451	69.15	19.19	43.57	50.19	0.31	2.46
442	68.24	19.38	42.39	50.46	0.30	2.56
433	64.24	19.01	38.89	49.05	0.29	2.66
424	54.26	17.05	31.53	43.34	0.27	2.61
415	50.64	17.29	27.59	42.91	0.24	2.99
406	47.31	15.27	26.96	38.53	0.26	2.42
550	57.03	18.19	32.78	46.06	0.27	2.84
541	50.68	17.14	27.83	42.66	0.24	2.92
532	56.75	18.68	31.85	46.87	0.25	3.05
523	56.79	17.25	33.79	44.23	0.28	2.51
510	56.26	17.61	32.78	44.81	0.27	2.67
505	52.06	14.17	33.17	37.21	0.31	1.77

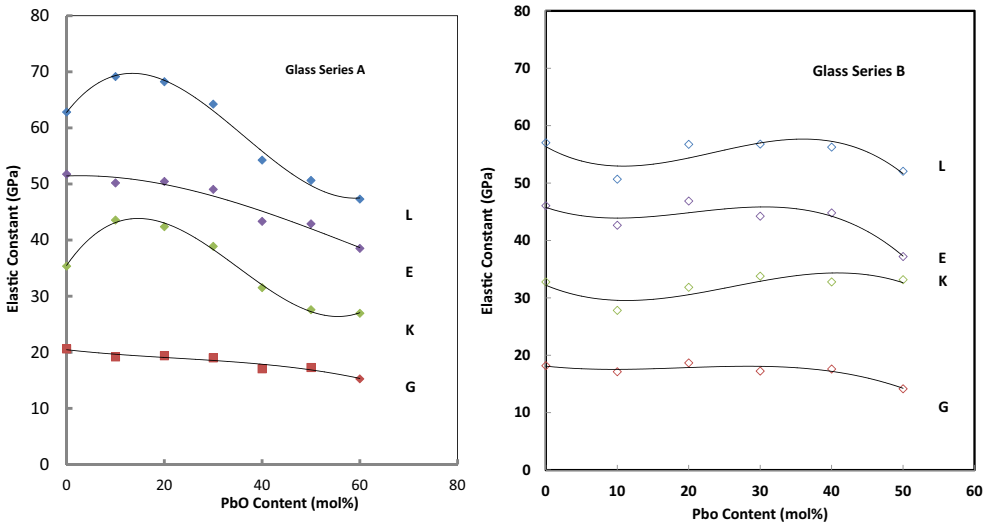

Fig. 3. The elastic constants (L, E, K and G) of A: $40(P_2O_5)$–$(60-x)$ZnO–xPbO – First Series (filled diamond) and B: $50(P_2O_5)$–$(50-x)$ZnO–xPbO – Second Series (open diamond).

greatly decreased with the crosslink density. This will lead to a decrease in glass rigidity. Density and molar volume increase with the addition of PbO in $(PbO)_x(P_2O_5)_{1-x}$ glass system [22]. The velocities (V_l and V_t) and elastic moduli longitudinal, shear, bulk, and Young's show gradually increasing trend as PbO is being added into the lead phosphate glass network while Poisson's ratio remains almost constant.

Microhardness of the glasses decreased from 3.35 to 2.42 and from 2.84 to 1.77 for glass A and glass B respectively as the content of PbO is increased. Although the glasses become softer, it is denser as the density increase in value. The present PbO–ZnO–P_2O_5 glass is in the range Young's modulus represented the stiffness of materials, which is related to the bonding strength between the greater the modulus, the stiffer is the material.

Theoretical analysis of elastic moduli

A comprehensive quantitative analysis of the experimentally determined elastic modulus systems of the $40(P_2O_5)$–$(60-x)$ ZnO–xPbO and $50(P_2O_5)$–$(50-x)$ZnO–xPbO where x = 0–60 mol% at room temperature has been carried out based on two theoretical models, namely bond compression model [25] and Makishima–Mackenzie model [26,27]. The prediction is based on (i) bond compression model which is based on the assumption that an isotropic deformation merely changes network bond lengths without changing in bond angles, (ii) Makishima–Mackenzie theory, which correlates the bulk modulus with packing density and dissociation energy per unit volume.

The bond compression model [25,26] provides the value of bulk modulus K_{bc}, number of bonds per unit volume n_b and $\bar{n}_c$ is the number of cross-links per unit cation which equals the number of bonds less than two as

$$k_{bc} = \sum_n \left(\frac{n_b r^2 F}{9}\right) \tag{9}$$

$$n_b = \sum_n \left(\frac{N_f N_A \rho}{M}\right) \tag{10}$$

and

$$\bar{n}_c = \frac{1}{\eta}\sum_i x_i (n_c)_i (N_c)_i \tag{11}$$

where x_i, is the mole fraction of component oxide, N_c the number of cations per unit glass formula, η is the total number of cations per unit glass formula unit given by

$$\eta = \sum_i x_i (N_c)_i \tag{12}$$

The average bond stretching force constant $\bar{F}$ is given by

$$\bar{F} = \frac{\sum (x n_f f)_i}{\sum (x n_f)_i} \tag{13}$$

where n_f is the coordination number of cation, and f is the stretching force constant of oxide. To complete the outlook of the structural geometry, two important parameters must be presented, they are, the estimated bulk modulus k_{bc} and the average ring size ℓ, which are given by

$$\ell = \left[0.0106 \frac{F}{K_e}\right]^{0.26} \tag{14}$$

where r is the bond length and F is the first order stretching force constant, K_e is the experimental bulk modulus. The theoretical Poisson's ratio for σ_{theo} the polycomponent oxide glasses according to the bond compression model is given by

$$\sigma_{theo} = 0.28(\bar{n}_c)^{-0.25} \tag{15}$$

The other elastic moduli can be obtained from bulk modulus and Poisson's ratio for each glass system as

Shear modulus:

$$G_{theo} = 1.5 K_{cal}\left[\frac{1-2\sigma_{theo}}{1+\sigma_{theo}}\right] \tag{16}$$

Longitudinal modulus:

$$L_{theo} = K_{bc} + 1.33 G_{theo} \tag{17}$$

Young's modulus:

$$E_{theo} = 2(1+2\sigma_{theo}) G_{theo} \tag{18}$$

Secondly, Makishima and Mackenzie [27,28] derived a semi-empirical formula model to calculate the elastic moduli of oxide glasses in terms of chemical composition, which depends only on the packing density (V_i) and dissociation energy (G_i) of the oxide constituents. The elastic moduli (Young's Modulus E, Bulk Modulus K, Shear Modulus G and Poisson's ratio σ) are given as follows:

Table 3A
Theoretical values of the average bond stretching force constant $\bar{F}$, the average ring size ℓ, number of bonds per unit volume n_b, number of cross-links per unit cation $\bar{n}_c$, calculated bulk modulus K_{bc}, ratio of (K_{bc}/K_e), theoretical Poisson's ratio σ_{theo}, theoretical shear G_{theo}, theoretical longitudinal L_{theo}, theoretical Young's E_{theo} according to bond compression and Young's, bulk, shear, dissociation energy, packing density and Poissons ratio E_m, K_m, G_m, G_i, V_t and σ_m according to Makishima model for glass A $40(P_2O_5)$–$(60-x)$ZnO–xPbO.

Glass A	$\bar{F}$	ℓ	n_b	$\bar{n}_c$	K_{bc}	K_{bc}/K_e	σ_{theo}	E_{theo}	G_{theo}	L_{theo}	E_m	K_m	G_m	G_i	V_t	σ_m
460	301.5	0.5348	10.48	3.429	110.3	3.12	0.2058	194.8	80.76	217.7	23.90	13.85	9.854	41.22	0.5797	0.2604
451	298.6	0.5052	10.79	3.286	112.8	2.589	0.208	197.7	81.83	221.7	24.49	15.47	9.905	38.76	0.6318	0.2802
442	295.5	0.5074	10.75	3.143	111.6	2.631	0.2103	193.9	80.1	218.1	24.20	16.13	9.680	36.30	0.6666	0.2917
433	292.2	0.5174	9.759	3.000	100.4	2.582	0.2128	173.1	71.35	195.3	21.71	13.93	8.753	33.84	0.6416	0.2835
424	288.6	0.5447	9.099	2.857	92.78	2.943	0.2154	158.5	65.19	179.5	19.93	12.66	8.052	31.38	0.6351	0.2813
415	284.7	0.562	8.584	2.714	86.67	3.141	0.2181	146.6	60.16	166.7	18.42	11.74	7.438	28.92	0.6370	0.282
406	280.4	0.5631	7.966	2.571	79.56	2.951	0.2211	133.1	54.51	152.1	16.65	10.48	6.742	26.46	0.6294	0.2793

Table 3B
Theoretical values of the average bond stretching force constant $\bar{F}$, the average ring size ℓ, number of bonds per unit volume n_b, number of cross-links per unit cation $\bar{n}_c$, calculated bulk modulus K_{bc}, ratio of (K_{bc}/K_e), theoretical Poisson's ratio σ_{theo}, theoretical shear G_{theo}, theoretical longitudinal L_{theo}, theoretical Young's E_{theo} according to bond compression and Young's, bulk, shear, dissociation energy, packing density and Poissons ratio E_m, K_m, G_m, G_i, V_t and σ_m according to Makishima model for glass B: $50(P_2O_5)$–$(50-x)$ZnO–xPbO.

Glass B	$\bar{F}$	ℓ	n_b	$\bar{n}_c$	K_{bc}	K_{bc}/K_e	σ_{theo}	E_{theo}	G_{theo}	L_{theo}	E_m	K_m	G_m	G_i	V_i	σ_{theo}
550	324	0.5557	9.425	3.333	101.6	3.099	0.2072	178.4	73.9	199.8	23.72	14.41	9.677	39.05	0.6074	0.2713
541	321.9	0.579	8.86	3.200	94.9	3.41	0.2093	165.5	68.42	185.9	22.07	13.31	9.017	36.59	0.6031	0.2697
532	319.7	0.558	9.04	3.067	96.19	3.02	0.2116	166.5	68.69	187.6	22.21	14.45	8.927	34.13	0.6507	0.2866
523	317.3	0.5483	8.457	2.933	89.34	2.644	0.214	153.3	63.16	173.3	20.41	13.15	8.221	31.67	0.6445	0.2845
510	314.6	0.5515	8.073	2.800	84.61	2.581	0.2165	143.9	59.17	163.3	19.05	12.42	7.654	29.21	0.6522	0.287
505	311.8	0.5485	7.193	2.667	74.74	2.253	0.2191	126	51.66	143.4	16.5	10.18	6.71	26.75	0.6170	0.2749

$$E_m = 2V_tG_t \tag{19}$$

$$K_m = \alpha V_tE \tag{20}$$

$$G_m = 3EK/(9K-E) \tag{21}$$

$$\sigma_m = (E/2G) - 1 \tag{22}$$

where V_t is the total packing density which is defined (the ratio between the minimum theoretical volume occupied by the ions and the corresponding ionic volume) as

$$V_t = \left(\frac{1}{V_m}\right)\sum_i (V_ix_i) \tag{23}$$

where V_m is the molar volume, x_i is mole fraction of the component i of an oxide glass, G_t is the total dissociation energy which is calculated from

$$G_t = \sum_i (G_ix_i) \tag{24}$$

Tables 3A and 3B collected the calculated values of the average bond stretching force constant $\bar{F}$, the average ring size ℓ, number of bonds per unit volume n_b, number of cross-links per unit cation $\bar{n}_c$, calculated bulk modulus K_{bc}, ratio of (K_{bc}/K_e), theoretical Poisson's ratio σ_{theo}, theoretical shear G_{theo}, theoretical longitudinal L_{theo}, theoretical Young's E_{theo} and Young's, bulk, shear, dissociation energy, packing density and Poissons ratio E_m, K_m, G_m, G_i, V_t and σ_m for both glass series A and for glass series B.

The calculated values of K_{bc} for prepared glasses are higher than the obtained experimental value K_{exp} as shown in Tables 2, 3A and 3B. The calculated bulk modulus (Bond Compression model K_{bc} decreases from 110.3 to 79.56 GPa, and the ratio (K_{bc}/K_{exp}) decreases from 3.12 to 2.951 with increasing of PbO content in glass A and also from 101.6 to 74.74 GPa, and the ratio (K_{bc}/K_{exp}) decreases from 2.099 to 2.253 for glass B. It can be seen that the ratio (K_{bc}/K_{exp}) forms a rough measure of the degree to which bond bending processes are involved in isotropic elastic deformation of the structure at room temperature. The increase in the theoretical average atomic ring diameter from 5.348 to 5.631 nm for glass series A and decrease from 5.557 to 5.485 nm

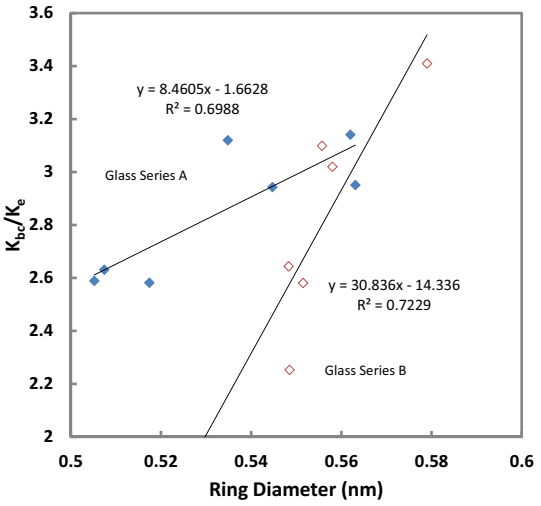

Fig. 4. Plot of the ratio (K_{bc}/K_{exp}) and atomic ring diameter for glass A: $40(P_2O_5)$–$(60-x)$ZnO–xPbO – First Series (filled diamond) and glass B: $50(P_2O_5)$–$(50-x)$ZnO–xPbO – Second Series (open diamond).

for glass series B as shown in Fig. 4. The increase in ℓ confirms the decrease in the experimental elastic moduli and therefore the network structure becomes more opened with increasing PbO as in glass A and opposite in glass B. The decrease in crosslink density $\bar{n}_c$ from 3.429 to 2.571 with increasing PbO content as shown for glass A and from 3.333 to 2.667 for glass B. Moreover, the number of network bonds per unit volume decreased from 10.48×10^{25} to 7.966×10^{25} m^{-3} and from 9.425×10^{25} to 7.193×10^{25} m^{-3} for glass A and glass B respectively. The average stretching force constant decreases from 301.5 to 280.4 and from 324.0 to 311.8 Nm^{-1} with increase of PbO content in both glass A and glass B, respectively. Theoretical Poisson's ratio increased from 0.2058 to 0.2211 and from 0.2072 to 0.2191 for both glass A and glass B. Theoretical shear, longitudinal and Young's modulus decreased with increasing the content of PbO in both glass A and glass B. Furthermore, the calculated values of the dissociation energy G_t of the present glass compositions were found to decrease from 41.22 to

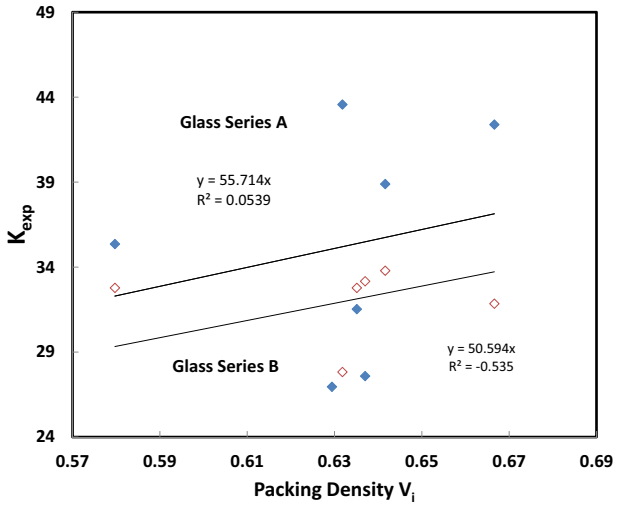

Fig. 5. Experimental bulk modulus against K_{exp} and the packing density V_i for glass A: $40(P_2O_5)$–$(60-x)$ZnO–xPbO – First Series (filled diamond) and glass B: $50(P_2O_5)$–$(50-x)$ZnO–xPbO – Second Series (open diamond).

26.46 and from 39.05 to 26.75 kJ cm^{-3} due to the increasing of PbO mol% in glass A and glass B, respectively. According to Makishima and Mackenzie [27,28], the packing density V_t increased from 0.5797 to 0.6294 and 0.6074 to 0.617 cm^3 mol^{-1} as in Tables 3A and 3B. The rest of the theoretical elastic moduli decreased while Poisson's ratio increased for glass series A and glass series B as in Tables 3A and 3B. Also, from the Tables 1 and 3, the value of packing density increases with increasing the concentration of PbO in $40(P_2O_5)$–$(60-x)$ZnO–xPbO and $50(P_2O_5)$–$(50-x)$ZnO–xPbO glasses. Bulk modulus is defined as the ratio between isotropic pressure and relative volume change. The value of bulk modulus measures resistance of the glass to the uniform compression. According to Makishima–Mackenzie theory [27,28] and also from earlier studies [29–32], tightly packed glasses have higher elastic moduli compared with loosely packed glasses. Fig. 5 represents the relationship between the experimental bulk modulus and the packing density for glass A and glass B. The forward proportionality between bulk modulus and packing density is in accordance with Makishima and Mackenzie [27,28] view. These results suggest that, the packing density is a tool of exploring the change in the mechanical properties of the glass. Fig. 6 summarizes both models for the interpretation of the elastic moduli. It is clear that the experimental points of the bulk modulus lie between both theoretical models; bond compressional and Makishima and Mackenzie models.

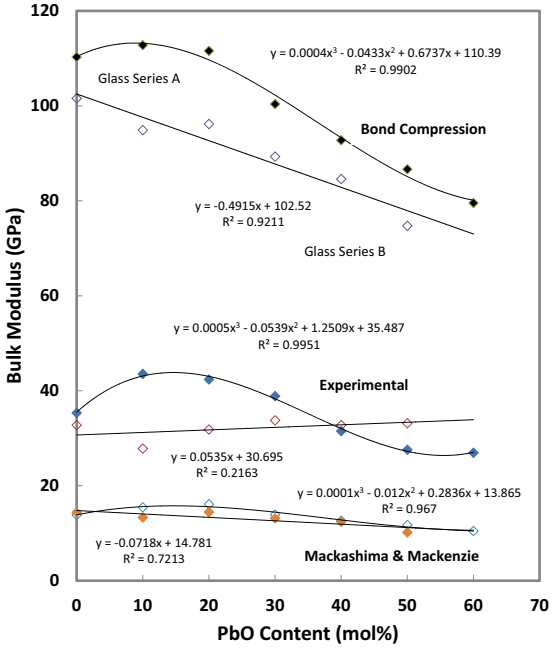

Fig. 6. Experimental bulk modulus K_{exp}, theoretical bulk modulus by compression model K_{bc} and theoretical bulk modulus by Makishima and Mackenzie models for glass A: $40(P_2O_5)$–$(60-x)$ZnO–xPbO – First Series (filled diamond) and glass B: $50(P_2O_5)$–$(50-x)$ZnO–xPbO – Second Series (open diamond).

Conclusions

Elastic properties studies on glass systems $40(P_2O_5)$–$(60-x)$ZnO–xPbO and $50(P_2O_5)$–$(50-x)$ZnO–xPbO where x = 0–60 mol% have been investigated to ascertain the effect of Pb^{2+} ion in these glasses. The densities show an increasing trend due an increase in PbO content and also due to the heavier Pb atoms. An increase in the density of the glasses accompanying the addition of PbO probably results in a change in crosslink density. The sound velocity and, elastic properties such as Young's modulus, bulk modulus, shear modulus, and longitudinal modulus decreased, while Poisson's ratio increased with PbO content. The increase in Poisson's ratio suggests that the rigidity of the glasses has decreased. Effect of PbO on the elastic behavior of ZnO–P_2O_5 glass systems has been discussed according of the average bond stretching force constant $\bar{F}$, the average ring size ℓ, the number of bonds per unit volume n_b, the number of cross-links per unit cation $\bar{n}_c$, the packing density (V_i) and dissociation energy (G_i) of the oxide constituents. The measured values of elastic constants and Poisson's ratio were found to be in between the theoretically calculated values of elastic moduli calculated by the bond compression and Makishima–Mackenzie models.

References

[1] Reis ST, Faria DLA, Martinelli JR, Pontuschka WM, Day DE, Partiti CSM, Non-Cryst J. Solids 2002;304:188.
[2] Sales BC, Ramsey RS, Bates JB, Boatner LA, Non-Cryst J. Solids 1986;87:137.
[3] Sales BC, Boatner LA. Science 1984;226:45.
[4] Poirier G, Poulain M, Poulain M, Non-Cryst J. Solids 2001;284:117.
[5] Dayanand C, Salagram M. Ceram Int 2004;30:1731.
[6] Subbalakshmi P, Veeraiah N. Phys Chem Glasses 2001;42:307.
[7] Prasad SVGVA, Sahaya Baskaran G, Veeraiah N. Phys. Status Solidi A 2005;202:2812.
[8] Durga DK, Veeraiah N. Ind J Pure Appl Phys 2001;39:382.
[9] Sahaya Baskaran G, Krishna Mohan N, Venkateswara Rao V, Krishna Rao D, Veeraiah N. Eur Phys J Appl Phys 2006;34:97–106.
[10] Subhalakshmi P, Veeraiah N. Mater Lett 2002;56:880.
[11] Altaf M, Chaudhry MA, Siddiqi SA. Glass Phys Chem 2005;31:597.
[12] Wasylak J, Kityk IV, Kucharski J. Phys Status Solidi A 2003;199:515.
[13] Kityk IV, Wasylak J, Benet S, Dorosz D, Kucharski J, Krasowski J, Sahraoui B. J Appl Phys 2002;92:2260.
[14] Wasylak J, Makowska-Janusik M, Sahraoui B, Dorosz D, Migalska- Zalas A, Imiolek W, Kucharski J, Krasowski J, Kityk IV, Plucinski KJ. Non-linear Opt 2002;29:99.
[15] Raghavaiah BV, Veeraiah N. J Phys Chem Solids 2004;65:1153; Raghavaiah BV, Laxmikanth C, Veeraiah N. Opt Commun 2004;235:341.
[16] Srinivasarao G, Veeraiah N. J Solid State Chem 2002;166:104; Srinivasarao G, Veeraiah N. Phys Status Solidi A 2002;191:370.
[17] Nassau K, Chadwick DL, Miller AE, Non-Cryst J. Solids 1987;93:115.
[18] Bishay A, Maghrabi C. Phys Chem Glasses 1969;10:1.
[19] Nassau K, Chadwick DL. J Am Ceram Soc 1982;65:197.
[20] Liu HS, Shih PY, Chin TS. Phys Chem Glasses 1996;37:227.
[21] Liu HS, Chin TS. Phys Chem Glasses 1997;38:123.
[22] Matori KA, Zaid MHM, Sidek HAA, Kamari HM, Wahab Zaidan Abdul. J Non-Cryst Solids 2013;361:78–81.
[23] Marzouk Samir Y. Mater Chem Phys 2009;114:188–93.
[24] El-Moneim Amin Abd. Phys B 2016;487:53–60.
[25] Bridge B, Higazy A. Phys Chem Glasses 1986;27:1–14.

[26] Lambson E, Saunders G, Bridge B, El-Mallawany R. J Non-Cryst Solids 1984;69:117–33.
[27] Makishima A, Mackenzie JD. J Non-Cryst Solids 1973;12:35.
[28] Makishima A, Mackenzie JD. J Non-Cryst Solids 1975;17:147.
[29] El-Mallawany R. J Appl Phys 1993;73:4878–80.
[30] El-Mallawany R, Sidkey M, Khafagy A, Afifi H. Mater Chem Phys 1994;37:295–8.
[31] El-Adawy A, El-Mallawany R. J Mater Sci Lett 1996;15:2065–7.
[32] El-Mallawany R. J Mater Res 1992;7:224–8.